Special relativity in the school laboratory: a simple apparatus for cosmic-ray muon detection

2015 Phys. Educ. 50 317

(http://iopscience.iop.org/0031-9120/50/3/317)

OPEN ACCESS

PAPERS

iopscience.org/ped

Special relativity in the school laboratory: a simple apparatus for cosmic-ray muon detection

P Singh[1] **and H Hedgeland**[1,2]

[1] The Perse School, Cambridge, CB2 8QF, UK

E-mail: h.hedgeland@ucl.ac.uk

Abstract

We use apparatus based on two Geiger–Müller tubes, a simple electronic circuit and a Raspberry Pi computer to illustrate relativistic time dilation affecting cosmic-ray muons travelling through the atmosphere to the Earth's surface. The experiment we describe lends itself to both classroom demonstration to accompany the topic of special relativity and to extended investigations for more inquisitive students.

1. Introduction

Special relativity was the subject of one of Albert Einstein's seminal papers of 1905, which played an important role in the foundation of modern physics [1]. However, the theory can often be perceived as too challenging for the school curriculum as the very high velocities required to observe significant relativistic effects have typically been outside the realm of school laboratory experiments. In this paper, we present a simple experiment by which the relativistic effect of time dilation is observed. Our apparatus uses two Geiger–Müller tubes, a simple electronic circuit and a Raspberry Pi computer to detect cosmic-ray muons. We illustrate an experimental approach which could be applied in a number of ways in the classroom, from a simple demonstration of relativistic effects, to an extended project that offers a keen student numerous avenues for the development of both their practical skills and theoretical understanding of topics in physics and mathematics, examples of which we detail here.

The theory of special relativity follows from just two postulates: that the laws of physics are the same in all inertial frames of reference and that the speed of light is constant in all inertial frames of reference. From these two postulates, Einstein derived several consequences. One of these is the effect of time dilation, memorable as 'moving clocks run slow'. Consider an object at the origin of reference frame S' moving with velocity v relative to reference frame S. In this case, time dilation is governed by the following equation:

$$\Delta t = \gamma \Delta t' = \frac{\Delta t'}{\sqrt{1 - \frac{v^2}{c^2}}} \tag{1}$$

where Δt is a time interval in S, $\Delta t'$ is the same interval in S' and γ is the Lorentz factor. This equation can be derived by considering light emitted from a moving object; it also follows as the inverse of the Lorentz transformation.

From equation (1), we observe that the magnitude of the time dilation effect depends on the

[2] Current address: London Centre for Nanotechnology, University College London, London, WC1H 0AH, UK.

velocity of the moving object relative to the speed of light; speeds close to the speed of light are required for time dilation to be measurable. We find objects with these speeds in naturally occurring cosmic rays.

Cosmic rays are high-energy particles that travel through interstellar space, striking the Earth's atmosphere at all times and from all directions. Although the mean rate of arrival of cosmic rays is anti-correlated to a small extent with the level of solar activity, which follows an approximately 11-year cycle, it appears effectively constant over measurements with timescales of days or weeks. It is known that the primary cosmic radiation consists of positively charged particles, largely protons and alpha particles. The energy spectrum of primary cosmic rays follows a power law in the range of 10^9–10^{20} eV [2]. These high energies correspond to cosmic ray particles having speeds very close to the speed of light.

When primary cosmic-ray particles strike the upper atmosphere, they undergo interactions with nuclei in the air resulting in the generation of pions. Pions have very short mean lifetimes and rapidly decay into muons, which make up the the majority of the cosmic radiation present at sea level. The muon is an unstable particle, undergoing exponential decay to electrons and neutrinos with a mean lifetime $\tau_\mu = 2.2\ \mu$s at rest [2]. This decay provides us with a 'clock' by which to observe time dilation.

2. Models for muon flux

Cosmic-ray muons are generated at a mean altitude of around 15 km [2]. Assuming they all travel with the upper limit of velocity, c, they can only travel 660 m in each mean lifetime of 2.2 μs. Without accounting for time dilation, this corresponds to the order of 1 in 10^{10} muons surviving the shortest (vertical) path to the surface.

Time dilation effectively extends the mean lifetimes of the muons, so that they are able to travel further in each mean lifetime in the Earth's frame of reference. Pfeffer and Nir [3] give the average speed of cosmic-ray muons as between $0.994c$ and $0.998c$. Using these values in equation (1) we find that the effective mean lifetime in our reference frame is extended to between 20.1 μs and 34.8 μs, corresponding to between 8% and 25% muons surviving the vertical path to the surface.

However, it is not enough to simply count how many muons we detect at sea level because we don't have an accurate figure for how many muons are being generated in the upper atmosphere. We can instead observe how their number varies over a known change in the distance they must travel. This is accomplished by measuring the flux of muons, $I(\theta)$, arriving at different angles, θ, to the vertical, having followed different path lengths through the atmosphere.

A mathematical derivation along with experimental measurements of some of the parameters have yielded the following accepted functional form for $I(\theta)$ [2, 4]:

$$I(\theta) \approx I(0)\ \cos^2\ \theta \qquad (2)$$

The derivation of this model relies on advanced mathematical analysis of the geometries of the Earth and the atmosphere. Below we present a simpler argument to justify the shape of this model and illustrate the need to take into account relativistic effects that students might like to reproduce for themselves as an exercise.

We must take into account two effects on the muons: their exponential decay and their interaction with the atmosphere. To simplify the geometry we first approximate the Earth to be flat, which is acceptable due to the small height of the atmosphere relative to the radius of the Earth and gives an error of less than 1% for $\theta < 70°$. Since they are charged particles, muons interact by ionization with the atoms in the air. The degree of attenuation through ionization is directly proportional to the length of the path that they travel; therefore the flux will be inversely proportional to the path length. Since the path length is inversely proportional to $\cos\theta$, $I(\theta) \propto \cos\theta$. Normalizing by the vertical path, the effect of the muons' interaction with the atmosphere can be modelled as $I(\theta)/I(0) = \cos\theta$.

As the muon's decay is exponential, equal fractions of some quantity of muons will decay in equal times. We can assume that the number of muons generated in the upper atmosphere is constant and uniform across the Earth and that their energy distribution is the same in all parts of the sky. Let the fraction of muons that survive the vertical path of 15 km be r $(0 < r < 1)$. Then after travelling a path k times longer than the vertical, the fraction that survive will be r^k. Using the same geometrical argument as previously, the fraction

of muons surviving the path at zenith angle θ will be $r^{1/\cos\theta}$. Therefore:

$$\frac{I(\theta)}{I(0)} = \frac{r^{1/\cos\theta}}{r} = r^{\frac{1}{\cos\theta}-1}$$

Combining these two effects yields the following approximation to the flux of muons at angle θ to the vertical:

$$\frac{I(\theta)}{I(0)} \approx r^{\frac{1}{\cos\theta}-1} \times \cos\theta \qquad (3)$$

Equation (3) is valid for any such exponential decay process and does not include or exclude the effect of time dilation; however, the value of r will be different in each case. If time dilation does not affect the muons, then $r \approx 10^{-10}$ as shown above. When we include the effect of time dilation, muons with different energies correspond to different values of r. We account for the energy spectrum of muons by using a range of values of r between 0.1 and 0.7; these correspond to muons with energies between about 1 GeV and 8 GeV. The resultant variation in normalized intensity with zenith angle θ is plotted as the green lines in figure 1(*a*).

From figure 1(*a*), it is clear that the accepted model of equation (2) (red line) is a good average approximation to the flux of cosmic-ray muons experiencing time dilation (green lines). However, it is not a good model for muons that are not experiencing time dilation, as shown by the curve of equation (3) with $r = 10^{-10}$ (light blue line). This sets up our experiment: we must measure the flux of cosmic-ray muons at different angles to the vertical and compare our results with the curves given by equations (2) and (3) to see whether time dilation has affected the muons in the way we predict.

3. Experimental apparatus

We now construct an apparatus that allows us to detect muons arriving at a particular known angle to the vertical. The apparatus must have high specificity, so that background radiation does not cause a systematic error. Below we describe a simple yet powerful technique for creating a directional muon detector: coincidence detection [2].

Cosmic-ray muons are ionizing radiation and so can be detected with instruments such as Geiger–Müller tubes and scintillation detectors. However, these instruments are not directional and will detect other background radiation. Carrying out the technique of coincidence detection overcomes both of these issues.

Coincidence detection involves orientating two detectors one above the other and observing when both trigger near-simultaneously—a coincidence event. Since the flux of background radiation is usually on the order of less than 1 detection per second, it is nearly certain that in a coincidence event the same particle has passed through and triggered both detectors. For practical purposes, a certain small time interval—the *coincidence window*—is chosen as the maximum temporal separation between two coincident events and a coincidence is recorded if events arrive from the two detectors separated by less than this window. With a suitable coincidence window the rate of spurious coincidences will be negligible compared to the observed coincidence rate. An interested student might like to calculate the rate of spurious coincidences using a Poisson distribution to model the triggering of each detector and examine the role of the coincidence window to confirm this statement.

This technique gives the apparatus the requisite directionality as any particle that causes a coincidence event must have originated in a certain cone of the sky defined by the shape of the detectors. This cone can be oriented to receive muons arriving at different zenith angles. The aperture of the cone depends on the separation of the detectors and may be calculated using simple trigonometry and the dimensions of the detector being used.

Coincidence detection also gives the detector specificity to cosmic-ray muons. At the surface of the Earth, the background radiation is mostly made up of alpha particles, beta particles and gamma rays, along with cosmic-ray muons. In order to block the terrestrial radiation, a few thin sheets of lead are placed between the two detectors. Almost no terrestrial alpha and beta particles are penetrating enough to trigger and exit one detector and pass through this lead shielding to reach the other detector. Gamma rays ionize matter via Compton scattering. However, these events are very rare; therefore the chance that one gamma ray will be able to pass through both the detectors and cause a Compton scattering event in each is negligible. So terrestrial background radiation is almost never able to cause a coincidence. On the other hand, cosmic-ray muons ionize continuously along their path and are very energetic, so they are easily able

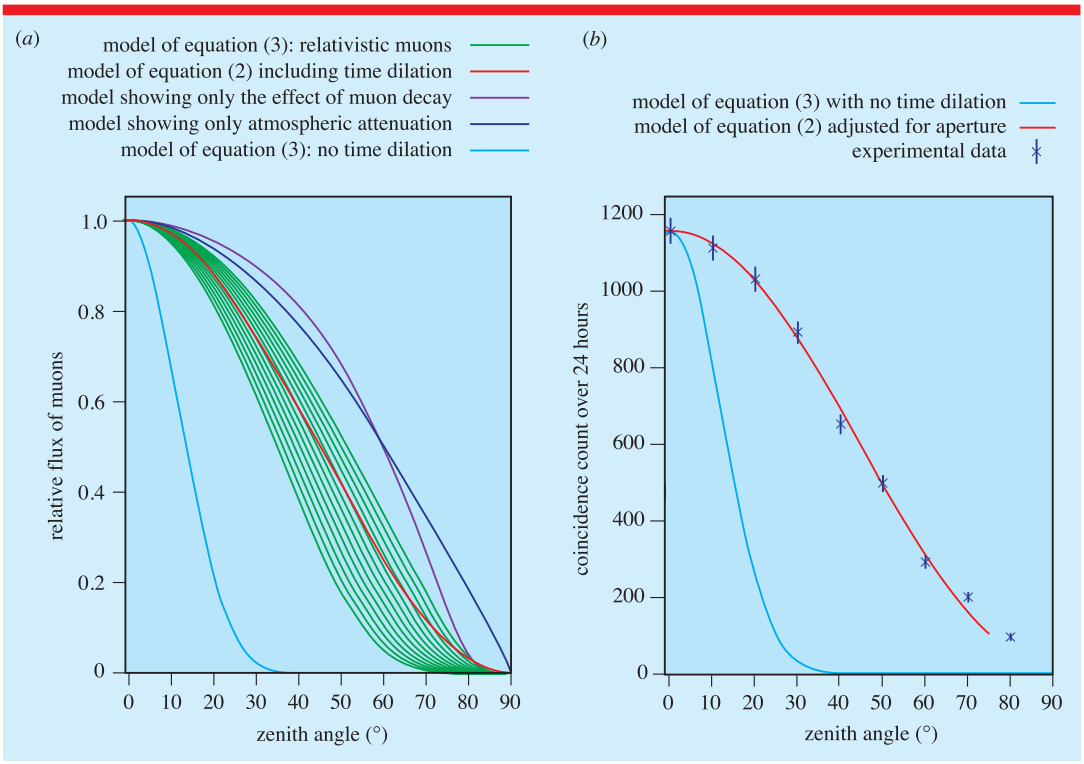

Figure 1. (*a*) Showing the curves described in section 2. The purple and dark blue curves illustrate only the effect of muon decay ($r = 0.5$) and atmospheric attenuation, respectively, whilst the green curves show both effects combined (equation (3)) for a range of relativistic muon energies ($r = 0.1, 0.15, 0.2...0.7$). The red curve shows the model of equation (2) which also accounts for special relativity. In contrast, the light blue curve shows the model of equation (3) with no time dilation ($r = 10^{-10}$). (*b*) Showing the measured dependence of the count on zenith angle in comparison with relativistic and non-relativistic models. Each data point represents a data-collection period of 24 h, with error bars of 1σ. The red curve shows the model of equation (2) adjusted for the size of the aperture, as described in section 4. The light blue curve is the model of equation (3) with $r = 10^{-10}$.

to pass through and trigger both detectors causing a coincidence event. Hence we can safely assume that all of the coincidence events that we observe are cosmic-ray muons.

We must now build an apparatus to carry out coincidence detection. Below we present two ways to do this. In both cases, we generalize our argument to allow for either GM tubes or scintillator-photomultiplier detectors to be used—we assume that we receive narrow voltage pulses from each detector when they are triggered. Diagrams of both systems are shown in figure 2.

3.1. Coincidence detection in hardware

We must build a system that triggers whenever pulses from the two detectors arrive within a certain small time interval of each other. We can build a circuit to do this.

The pulses from the detectors may be too narrow to visibly flash an LED, but they can be widened by using a standard monostable 555 timer circuit. The 555 IC is triggered by a fast bipolar-junction transistor such as the 2N3904 [5]. The output pulse will have a width of $1.1RC$ s, where R and C are the resistance and capacitance in the RC circuit connected to DIS and THR. This output pulse may be used to flash an LED or drive a counter.

This circuit can be easily modified by connecting two bipolar-junction transistors in series to the signals from the two detectors. This circuit is illustrated in figure 2(*a*). In this arrangement, the 555 monostable circuit will only be triggered when overlapping pulses arrive from the two detectors—i.e. a coincidence has taken place.

If necessary, two similar 555 monostable circuits may be used to first widen the raw pulses from the detectors before they arrive at the

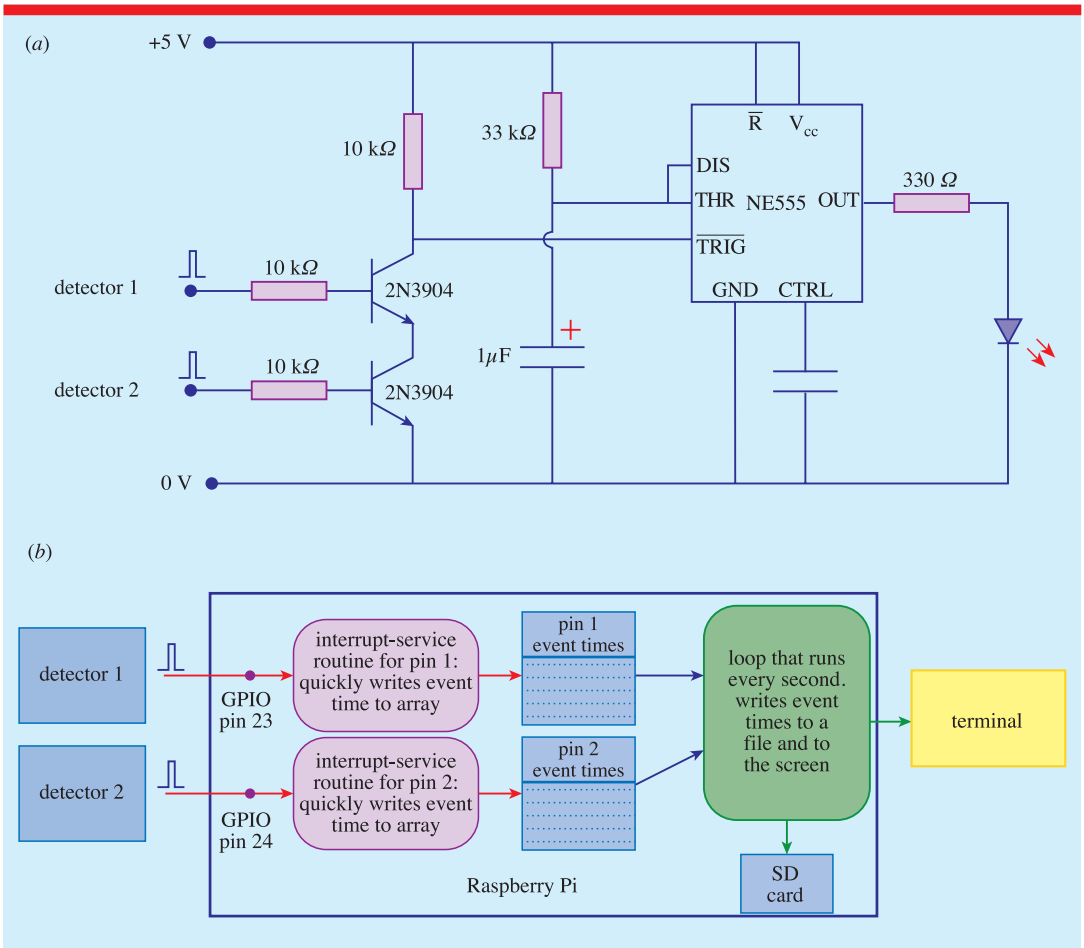

Figure 2. (*a*) Circuit diagram of the hardware coincidence system based on a 555 timer monostable circuit, as described in section 3.1. The resistor and capacitor values are those used by the authors. (*b*) Schematic diagram showing the flow of information in the software coincidence system running on a Raspberry Pi computer, as described in section 3.2.

coincidence circuit, to effectively increase the coincidence window of the circuit. Optionally, two LEDs may be placed at the outputs of these monostable circuits, so that individual events on the two detectors can also be observed.

3.2. Coincidence detection in software

We can also carry out coincidence detection in software. In order to do this, we need to deliver the pulses from the two detectors to a program running on the computer. We found the Raspberry Pi computer ideal for this purpose, because of its GPIO port. This has 26 pins, to 7 of which any 3.3 V digital input can be directly connected and whose state (ON/OFF) or a change of whose state (rising/falling edge) may be read in software. Other advantages of the Raspberry Pi include its easy programmability, low power consumption and small size.

Firstly, we carefully measure the voltage of the pulses from the detectors and construct a simple potential divider circuit using two resistors to reduce the pulse voltages to 3.3 V. We then feed these signals to two of the GPIO pins. Next, we need to trigger some processing whenever a pulse arrives on either of these two pins. We can do this using *interrupt-service routines*: small sets of instructions that are registered with the operating system and attached to certain events in the computer. As soon as an event occurs, any interrupt-service routines attached to it are run immediately. Since they are run at such a high priority,

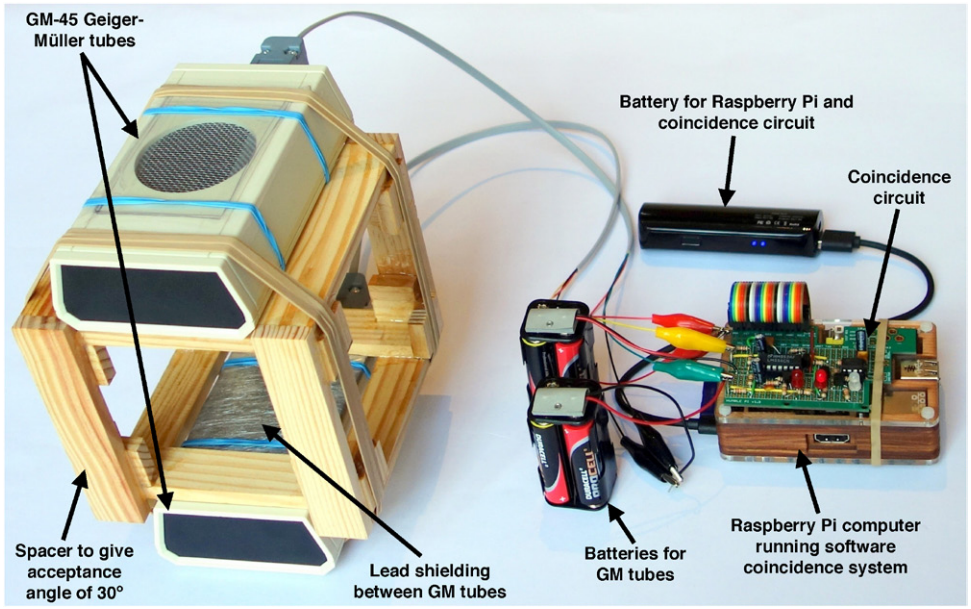

Figure 3. Labelled photograph of the apparatus used. The software coincidence system ran on the Raspberry Pi, while the hardware coincidence system was implemented on the circuit board on top of it.

interrupt-service routines need to carry out as little processing as possible and quickly return control to the operating system.

We wrote software for the Raspberry Pi to carry out coincidence detection, using the open-source 'wiringPi' library [6] to attach interrupt-service routines to rising-edge events on two of the GPIO pins. Each interrupt-service routine simply writes the time at which it triggered into an array in memory. A separate loop, running at lower priority and executing once every second, reads through all the times in memory added since it last checked and writes them to a file and to the screen.

Coincidence detection now consists of simply looking at pairs of neighbouring event times on opposite pins in memory and checking if their time separation is less than or equal to the specified coincidence window. This procedure can be carried out either during runtime by the lower priority loop, or after data collection is complete via post-processing the data file. The software coincidence system is illustrated by figure 2(*b*).

4. Analysis of results

We built both coincidence systems outlined in section 3 and using them constructed a directional cosmic-ray muon detector. The two systems run separately and in parallel, with the software system used primarily for data collection and the hardware system to get immediate information about detections and coincidences. In our apparatus, GM-45 Geiger–Müller tubes [7] from Black Cat Systems were used to detect radiation. The full experimental apparatus is shown in figure 3.

During data collection, the detectors were separated by the spacer shown in figure 3. This spacer set the acceptance angle of the detector to 30°. In order to compensate for this aperture, the model of equation (2) shown in figure 1(*b*) is slightly adjusted such that the value of the model at zenith angle θ is the average of the values of $\cos^2\theta$ in an interval from $\theta - 15°$ to $\theta + 15°$. The models are normalized by scaling by $I(0)$, the coincidence count at zenith angle 0°. The raw experimental data are also given in appendix A, table 1.

The apparatus was oriented at zenith angles ranging from 0° to 80° and coincidence counts were recorded for 24 h at each zenith angle. This duration was chosen so that any possible effect of the the time of day on the flux of cosmic rays would not affect the results.

Figure 1(*b*) shows that the results follow the model of equation (2) very well. Five out of the eight data points lie within 1 standard deviation of

the model that includes the effect of time dilation. The data clearly does not fit the model of equation (3) when it does not include the effect of time dilation.

In conclusion, the dependence of the observed muon flux on zenith angle shows a good fit to the model that includes the effect of relativistic time dilation. Hence we have experimentally observed a prediction of the theory of special relativity, using an apparatus that is inexpensive and widely applicable within the school laboratory. The approach offers numerous avenues for extension to students seeking to carry out independent investigations or progress to more advanced topics of study.

Received 30 September 2014, in final form 20 February 2015, accepted for publication 26 February 2015
doi:10.1088/0031-9120/50/3/317

Appendix A.

Table A1. Angular flux of cosmic-ray muons with detector acceptance angle 30°, as illustrated in figure 1(*b*).

Zenith angle θ/°	Observed count on GM tube 1/per 24 h	Observed count on GM tube 2/per 24 h	Observed coincidence count/ per 24 h	Standard deviation of observed coincidence count/ per 24 h
0.0	57 460	62 755	1162	34.09
10.0	57 285	62 467	1117	33.42
20.0	58 162	62 330	1035	32.17
30.0	57 179	61 880	895	29.92
40.0	55 259	60 590	654	25.57
50.0	52 916	58 640	498	22.32
60.0	51 616	57 098	291	17.06
70.0	50 857	56 068	199	14.11
80.0	49 808	55 605	95	9.75

References

[1] Einstein A 1905 Zur Elektrodynamik bewegter Körper *Ann. Phys., Lpz.* **17** 891
[2] Rossi B 1948 Interpretation of cosmic-ray phenomena *Rev. Mod. Phys.* **20** 537
[3] Pfeffer J I and Nir S 2000 *Modern Physics: an Introductory Text* (London: Imperial College Press)
[4] Kempa J and Brancus I M 2003 Zenith angle distributions of cosmic ray muons *Nucl. Phys.* B **122** 279
[5] Datasheet for the 2N3904 NPN general purpose amplifier, from Fairchild Semiconductor www.fairchildsemi.com/ds/2N/2N3904.pdf
[6] WiringPi library for Raspberry Pi http://wiringpi.com/
[7] Datasheet for the Black Cat Systems GM-45 detector www.blackcatsystems.com/GM/products/GM45GeigerCounter.html

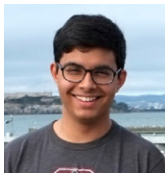

Pratap Singh is a student at The Perse School in Cambridge in the UK.

Holly Hedgeland is a Leverhulme Trust Early Career Fellow at University College London and a former teacher of mathematics and physics at The Perse School in Cambridge.